

One-Tap Equalizer for Perfect Reconstruction DFT Filter Bank Transceivers

François D. Beaulieu* and Benoît Champagne

Dept. of Electrical and Computer Engineering, McGill University

3480 University St, Montréal, Québec, H3A 2A7, Canada

Email: francois.duplessis-beaulieu@mail.mcgill.ca, benoit.champagne@mcgill.ca

Abstract—In this paper, we investigate a simple equalization method for DFT filter bank transceivers. We assume the presence of perfect reconstruction (PR) DFT filter banks and make use of this property to derive a one-tap per subcarrier equalizer. The proposed equalizer does not require additional bandwidth, other than the bandwidth necessary for PR purposes. Computer experiments show that the one-tap PR DFT filter bank transceiver outperforms the well-known OFDM system, especially in environments dominated by narrowband noise.

Index Terms—multicarrier modulation, DFT filter banks, equalizers.

I. INTRODUCTION

Multicarrier systems are now becoming more and more ubiquitous with their presence in many communication standards. For example, multicarrier systems are currently deployed in wireless Internet routers (Wi-Fi), high-definition television tuners (DVB) and digital subscriber line modems (DSL). The wide adoption of multicarrier systems can be explained in part by its robustness against ISI and multipath fading. These systems essentially employ the FFT to modulate several subcarriers in parallel and rely on a so-called cyclic prefix and a one-tap per subcarrier equalizer to combat intersymbol interference (ISI), a scheme known as orthogonal frequency-division multiplexing (OFDM) in wireless systems or as discrete multitone (DMT) in wireline applications (e.g. DSL).

However, due to the substantial overlap between adjacent subcarriers, OFDM/DMT suffers from poor spectral selectivity, making it rather sensitive to impairments such as narrowband noise. Fortunately, the combination of the FFT and cyclic prefix is not the only possibility for multicarrier systems and the use of wavelet or filter bank theory has proven to be a viable alternative [1], [2]. In this work, we focus on the equalization of DFT filter bank transceivers. Decision-feedback equalization [3], [4] and zero-padding combined with block linear equalization [2], [5], [6] are two popular equalization methods suitable for these transceivers. Unfortunately, the computational complexity of both methods is much higher than that of OFDM/DMT. The zero-padding scheme also necessitates extra bandwidth, like the cyclic prefix in OFDM/DMT, in addition to any bandwidth necessary for perfect reconstruction (PR) purposes.

We thus propose an equalization method for DFT filter bank transceivers that alleviates the aforementioned issues.

We assume the presence of PR DFT filter banks [7] and make use of this property to derive a one-tap per subcarrier equalizer. The proposed equalizer enjoys the same low per-subcarrier computational complexity as the one employed in OFDM/DMT. Contrary to the cyclic prefix and zero-padding, no extra bandwidth is necessary, other than the bandwidth normally required for PR. In order to ensure proper ISI cancellation, our equalizer operates under the assumptions that the number of subcarriers must be high enough (so that the subchannel frequency response is approximately flat) and that the stopband energy of the prototype filter is low (so that the interference between adjacent subcarriers is small). Simulations presented in this paper show that these assumptions can easily be satisfied in practice. Results also indicate that the one-tap PR DFT filter bank transceiver outperforms the OFDM system, especially in environments dominated by narrowband noise.

II. BACKGROUND

A typical filter bank multicarrier transceiver is illustrated in Fig. 1. This particular system transmits at a given rate M symbols $x_0[n], \dots, x_{M-1}[n]$ in parallel, which are first processed by the transmitting filter bank. K -fold upsampling is performed, followed by filtering by $F_i(z) = \sum_{m=0}^{D-1} f_i[m]z^m$, $i = 0, \dots, M-1$, where $f_i[m]$ are the filter coefficients and D is the filter length. We have chosen to express $F_i(z)$ as a noncausal filter for symmetry reasons that will become evident later, as we discuss paraunitary matrices. The resulting time-domain samples are then added together and sent through a channel, modelled here by a finite impulse response (FIR) filter $C(z) = \sum_{m=0}^{Q-1} c[m]z^{-m}$, where $c[m]$ is the channel impulse response and Q represents its length. These samples are then contaminated by an additive noise $\eta[m]$. Demodulation is carried out by the receiving filter bank, i.e. an array of M filters $H_i(z) = \sum_{m=0}^{D-1} h_i[m]z^{-m}$, $i = 0, \dots, M-1$, where $h_i[m]$ are the filter coefficients, followed by K -fold decimators. Finally, the received symbols are equalized via single taps e_0, \dots, e_{M-1} , yielding the received symbols $y_0[n], \dots, y_{M-1}[n]$.

The multirate system illustrated in Fig. 1 can be conveniently represented using the so-called polyphase notation and relevant multirate properties [8]. The equivalent system is shown in Fig. 2. The (k, i) -th entry of the $K \times M$ polynomial matrix $G(z)$ corresponds to a polyphase component of $F_i(z)$,

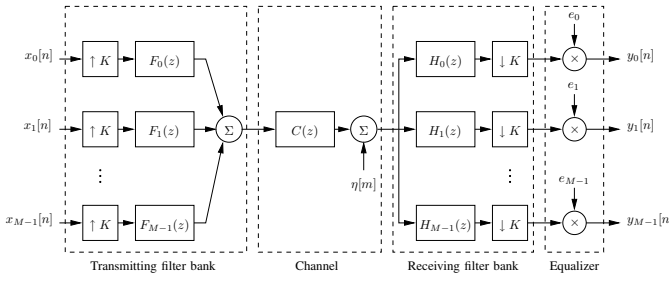


Fig. 1. A filter bank transceiver with a one-tap per subcarrier equalizer.

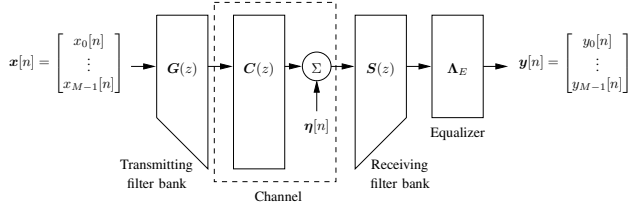


Fig. 2. Filter bank transceiver represented using the polyphase notation.

i.e.

$$[\mathbf{G}(z)]_{k,i} = \sum_{n=0}^{D/K-1} f_i[Kn+k]z^n. \quad (1)$$

Similarly, the $M \times K$ polynomial matrix $\mathbf{S}(z)$ is given by

$$[\mathbf{S}(z)]_{i,k} = \sum_{n=0}^{D/K-1} h_i[Kn+k]z^{-n}.$$

Provided that $Q \leq K$, the channel matrix $\mathbf{C}(z)$ can be expressed as follows:

$$\mathbf{C}(z) = \mathbf{C}_0 + \mathbf{C}_1 z^{-1},$$

where \mathbf{C}_0 is a lower triangular Toeplitz matrix whose first column is given by $[c[0] \ \dots \ c[Q] \ 0 \ \dots \ 0]^T$ and \mathbf{C}_1 is an upper triangular Toeplitz matrix whose first row is given by $[0 \ \dots \ 0 \ c[Q] \ \dots \ c[1]]$ [5]. Noise is now represented by a vector $\boldsymbol{\eta}[n]$, i.e.

$$\boldsymbol{\eta}[n] = [\eta[Kn] \ \eta[Kn+1] \ \dots \ \eta[Kn+K-1]]^T,$$

and the one-tap equalization can be expressed as a diagonal matrix as follows:

$$\boldsymbol{\Lambda}_E = \text{diag}(e_0, \dots, e_{M-1}).$$

Perfect reconstruction (PR) filter banks are a class of filter banks that satisfies $\mathbf{S}(z)\mathbf{G}(z) = z^{-d}\mathbf{I}_M$, where d is some fixed integer delay. In a transceiver application, such property is highly desirable, as it eliminates the need to compensate for distortion introduced by the filter banks themselves. PR can be satisfied by enforcing $\mathbf{G}(z)$ to be a paraunitary matrix, that is, a matrix characterized by the property $\tilde{\mathbf{G}}(z)\mathbf{G}(z) = \mathbf{I}_M$, where the tilde represents the paraconjugation operator, i.e. $\tilde{\mathbf{G}}(z) = \mathbf{G}^H(1/z^*)$. In this case, the receiving filter bank can be completely derived from the transmitting filter bank, $H_i(z) = F_i^*(1/z^*)$ [8].

III. DFT FILTER BANKS

DFT filter banks rely on a complex modulation to derive their filters $F_i(z)$, $i = 0, \dots, M-1$, i.e.

$$F_i(z) = F_0(zW^i), \quad (2)$$

where $W = e^{-j2\pi/M}$. $F_0(z)$ represents a so-called prototype filter and must be designed appropriately if we want $\mathbf{G}(z)$ to be paraunitary. In this paper, we follow the method proposed in [7]. Compared to non-modulated filter banks, DFT filter banks are advantageous because of their reduced design complexity (only one filter, $F_0(z)$, must be designed instead of M). Moreover, the modulation can be implemented efficiently via the FFT algorithm.

In the case of DFT filter banks, $\mathbf{G}(z)$ can be factorized as described here, using the ideas presented in [9]. Such factorization will be used in Section IV, where the one-tap equalizer is derived. Let $\mathbf{g}_i(z)$ be the i -th column of $\mathbf{G}(z)$. From (1), $\mathbf{g}_i(z)$ can be expressed as

$$\mathbf{g}_i(z) = \tilde{\mathbf{L}}_0(z) \begin{bmatrix} f_i[0] \\ \vdots \\ f_i[D-1] \end{bmatrix},$$

where $\tilde{\mathbf{L}}_0(z) = [\mathbf{I}_K \ z\mathbf{I}_K \ \dots \ z^{\frac{D}{K}-1}\mathbf{I}_K]$. Using the fact that $f_i[n]$ is a modulated filter and $W^{M+d} = W^d$, we can write

$$\mathbf{g}_i(z) = \tilde{\mathbf{L}}_0(z)\boldsymbol{\Lambda}_f\mathbf{L}_1^T \begin{bmatrix} W^{-0i} \\ \vdots \\ W^{-(M-1)i} \end{bmatrix}, \quad (3)$$

where $\boldsymbol{\Lambda}_f = \text{diag}(f_0[0], \dots, f_0[D-1])$ and

$$\mathbf{L}_1 = \underbrace{[\mathbf{I}_M \ \mathbf{I}_M \ \dots \ \mathbf{I}_M]}_{D/M \text{ times}}.$$

Finally, from (3), $\mathbf{G}(z)$ can be factorized as follows:

$$\mathbf{G}(z) = [\mathbf{g}_0(z) \ \dots \ \mathbf{g}_{M-1}(z)] = \tilde{\mathbf{L}}_0(z)\boldsymbol{\Lambda}_f\mathbf{L}_1^T\mathbf{W}^*,$$

where \mathbf{W} is the DFT matrix, i.e. $[\mathbf{W}]_{i,k} = W^{ik}$.

By defining $\mathbf{U}(z) \triangleq \mathbf{L}_1\boldsymbol{\Lambda}_f\mathbf{L}_0(z)$, $\mathbf{G}(z)$ can also be expressed as

$$\mathbf{G}(z) = \tilde{\mathbf{U}}(z)\mathbf{W}^*. \quad (4)$$

Let us consider $M \times K$ matrices \mathbf{F}_l , $l = 0, \dots, D/K-1$ as a partition of $\mathbf{L}_1\boldsymbol{\Lambda}_f$, i.e.

$$[\mathbf{F}_0 \ \dots \ \mathbf{F}_{D/K-1}] = \mathbf{L}_1\boldsymbol{\Lambda}_f.$$

Then, the matrix $\mathbf{U}(z)$ in (4) can be written as

$$\mathbf{U}(z) = [\mathbf{F}_0 \ \dots \ \mathbf{F}_{D/K-1}]\mathbf{L}_0(z) = \sum_{l=0}^{D/K-1} \mathbf{F}_l z^{-l}. \quad (5)$$

The factorization obtained in (4) and (5) is fundamental to the derivation of the one-tap per subcarrier equalizer, as explained in Section IV. Note that PR is possible only if $K > M$ [7], which we assume throughout this paper.

IV. ONE-TAP EQUALIZER

In this section, we derive an expression for the one-tap equalizer depicted in Figs. 1 and 2. In doing so, we must distinguish between two types of ISI, namely, intrablock ISI and interblock ISI. To define these two types of ISI, let us consider the noise-free transfer function of the system shown in Fig. 2, i.e.

$$\mathbf{T}(z) = \mathbf{\Lambda}_E \mathbf{S}(z) \mathbf{C}(z) \mathbf{G}(z) = \sum_l \mathbf{T}_l z^{-l}. \quad (6)$$

Intrablock ISI occurs when the off-diagonal entries of \mathbf{T}_d are not zeros, i.e. when the symbols within a block interfere with each other. Here, d represents the overall delay induced by the transceiver (due to internal processing delays). Interblock ISI is present when the symbols from a previous block interfere with those of the current received block or, in other terms, when $\mathbf{T}_l \neq \mathbf{0}$ for $l \neq d$. To achieve the PR property, a system must be free of intrablock and interblock ISI, i.e. $\mathbf{T}(z) = z^{-d} \mathbf{I}_M$.

Even though we employ PR DFT filter banks, i.e. $\tilde{\mathbf{G}}(z) \mathbf{G}(z) = \mathbf{I}_M$, we need to emphasize the fact that with $\mathbf{S}(z) = \tilde{\mathbf{G}}(z)$, $\mathbf{T}(z)$ does not generally satisfy the PR property, due to the term $\mathbf{C}(z)$ in (6). PR filter banks are still an asset since we do not have to be concerned with any distortion originating from the filter banks themselves. Note that if the spectral characteristics of the prototype filter $F_0(z)$ are good¹, the intrablock ISI should be negligible. Likewise, if the number of subcarriers M is large, then the subchannel frequency response should be almost flat, which would make the interblock ISI very small. Under these conditions, a one-tap per subcarrier equalizer would be sufficient to properly equalize the received symbols. The overall system would then be characterized by the near-PR property, i.e. $\mathbf{T}(z) \approx z^{-d} \mathbf{I}_M$. Note that non-PR filter banks would contribute to interblock ISI, making the subchannel frequency response non-flat and a one-tap per subcarrier equalizer unsuitable [4].

In order to compute the coefficient e_i , $i = 0, \dots, M-1$, of the one-tap per subcarrier equalizer, the transfer function (6) must be given explicitly. The transfer function can be written as

$$\mathbf{T}(z) = \mathbf{\Lambda}_E \mathbf{R}(z),$$

where

$$\mathbf{R}(z) = z^{-\frac{D}{K}+1} \mathbf{W} \mathbf{U}(z) (\mathbf{C}_0 + \mathbf{C}_1 z^{-1}) \tilde{\mathbf{U}}(z) \mathbf{W}^*. \quad (7)$$

Note that we have added a delay of $D/K-1$ in (7) to make the transmitter causal. Substituting (5) in (7) yields

$$\mathbf{R}(z) = \mathbf{W} \left(\sum_{p=0}^{D/K-1} \mathbf{F}_p z^{-p} \right) (\mathbf{C}_0 + \mathbf{C}_1 z^{-1}) \cdot \left(\sum_{q=0}^{D/K-1} \mathbf{F}_{\frac{D}{K}-1-q} z^{-q} \right) \mathbf{W}^*. \quad (8)$$

¹By good spectral characteristics, we refer to a filter having a sharp transition band, high out-of-band rejection, etc.

M	K	SIR_{inter} (dB)
32	36	2.52
48	54	4.03
64	72	5.66
96	108	8.03
128	144	9.66

TABLE I
SIGNAL-TO-INTERBLOCK ISI RATIO FOR DIFFERENT NUMBER OF SUBCARRIERS M , $D = 27M$.

We can re-arrange (8) as follows

$$\mathbf{R}(z) = \sum_{l=0}^{2D/K-1} \mathbf{R}_l z^{-l},$$

where

$$\mathbf{R}_l = \mathbf{W} \left(\sum_{p=0}^{D/K} \mathbf{F}_{l-p} \left(\mathbf{C}_0 \mathbf{F}_{\frac{D}{K}-p-1}^T + \mathbf{C}_1 \mathbf{F}_{\frac{D}{K}-p}^T \right) \right) \mathbf{W}^*, \quad (9)$$

with $\mathbf{F}_l = \mathbf{0}$ for $l < 0$ and $l > D/K-1$.

The one-tap coefficients can be found by using (9). A zero-forcing approach yields

$$e_i = \frac{1}{[\mathbf{R}_d]_{i,i}}$$

where d is the inherent delay of the transceiver. The computational complexity of this equalizer is very low, requiring only one complex multiplication per symbol — or 6 flops — which is exactly the same level of complexity found in OFDM/DMT. The assumptions about the intrablock and interblock ISI will be verified in the next section.

V. COMPUTER EXPERIMENTS

Results presented in this section are obtained for a channel $\mathbf{C}(z)$ representing a 100-metre twisted-pair UTP-3 cable, commonly encountered in traditional telephony systems. For simulation purposes, we approximate the magnitude of the frequency response of such cable, given in [3], by a 17-tap FIR filter using a least square approach. The prototype filters $F_0(z)$ are designed using the PR method proposed in [7].

Recall that, to operate properly, a one-tap per subcarrier equalizer can only tolerate a small amount of interblock and intrablock ISI. As stated in Section IV, if M is large enough, the subchannel frequency response should be approximately flat, which, in turn, should make the interblock ISI negligible. Table I gives the signal-to-interblock ISI ratio for different values of M . The signal to interblock ISI ratio (SIR_{inter}) is obtained via

$$SIR_{\text{inter}} = 10 \log_{10} \left(\frac{\|\text{diag}(\mathbf{R}_d)\|_2^2}{\sum_{l=0, l \neq d}^{2D/K-1} \|\mathbf{R}_l\|_F^2} \right),$$

where \mathbf{R}_l is given in (9). As M increases, we note that SIR_{inter} also increases, which implies that the interblock ISI power decreases. Our assumptions about the interblock ISI are thus valid.

E_{sb}	SIR_{intra} (dB)
0.4712	6.47
0.2402	9.03
0.0578	11.0
0.0040	12.7
0.0006	15.4

TABLE II
SIGNAL-TO-INTRABLOCK ISI RATIO FOR A SYSTEM WITH $M = 128$,
 $K = 144$, AND $D = 27M$.

We next compute the signal-to-intrablock ISI ratio, SIR_{intra} , for a system with $M = 128$, $K = 144$ and $D = 27M$. SIR_{intra} is obtained using

$$SIR_{intra} = 10 \log_{10} \left(\frac{\|\text{diag}(\mathbf{R}_d)\|_2^2}{\|\mathbf{R}_d - \text{diag}(\mathbf{R}_d)\|_F^2} \right).$$

Several prototype filters are used, each of them characterized by a different amount of stopband energy. We have hypothesized in Section IV that a good spectral selectivity should make SIR_{intra} relatively small, since adjacent subcarriers will not interfere with each other. We measure the spectral selectivity by normalizing the stopband energy of the prototype filter by the total energy of the filter, i.e.

$$E_{sb} = \frac{\int_{\pi/M}^{\pi} |F_0(e^{j\omega})|^2 d\omega}{\int_0^{\pi} |F_0(e^{j\omega})|^2 d\omega}.$$

The spectral selectivity is thus improved as E_{sb} approaches 0. Results can be found in Table II. Table II confirms the fact that the intrablock ISI power decreases as the spectral selectivity improves.

Whether the interblock and intrablock ISI can be termed “negligible”, so that the one-tap per subcarrier equalizer can operate properly, remains to be assessed. We consider a one-tap PR DFT filter bank system with $M = 128$, $K = 144$ and $D = 27M$. By comparing the performance of the proposed transceiver and the conventional 128-subcarrier OFDM system, we will be able to determine if the one-tap equalizer is operating in a satisfactory manner. The performance is evaluated in terms of achievable bit rates, given by [3]

$$R = \frac{f_s}{K} \sum_{m=0}^{M-1} \left[\log_2 \left(1 + \frac{\sigma_{x,m}^2 SNR_m \gamma_{code}}{\Gamma \gamma_{margin}} \right) \right],$$

where f_s is the sampling frequency in Hz, $\sigma_{x,m}^2$ is the power allocated to subcarrier m , SNR_m is the subchannel SNR, γ_{code} is the coding gain, γ_{margin} is the additional noise margin, and Γ is the SNR gap, representing the difference between the modulation scheme (e.g. QAM) and channel capacity for a given error probability. In our experiments, we select $f_s = 22.08$ MHz, $\gamma_{code}/\gamma_{margin} = 1$ and $\Gamma = 9.8$ dB (corresponding to an error probability of 10^{-7}).

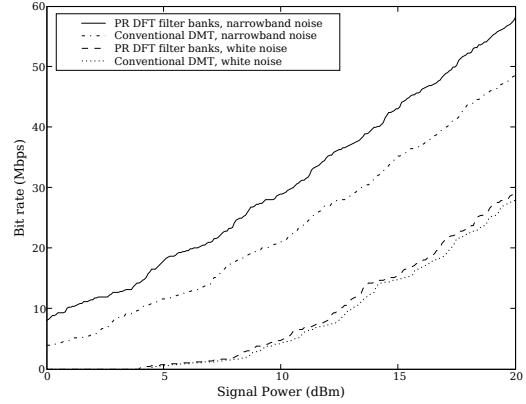


Fig. 3. Achievable bit rates of the PR DFT filter bank transceiver with one-tap equalization, and of the OFDM system.

Results are presented in Fig. 3 and are obtained for two different noisy environments. An additive white Gaussian noise, characterized by a flat power spectral density (PSD) of -77 dBm/Hz, and a narrowband noise are employed. The narrowband noise is generated using a second-order autoregressive process whose poles are $0.9995e^{\pm 1.6j}$. In both cases, the proposed transceiver outperforms the OFDM system, implying that the one-tap equalizer is indeed working correctly and that the interblock and intrablock ISI are sufficiently small. The performance improvement becomes quite significant when narrowband noise contaminates the system. This behaviour is due to the fact that DFT filter banks offer a much better spectral selectivity than OFDM.

REFERENCES

- [1] A. Jamin and P. Mähönen, “Wavelet packet modulation for wireless communications,” *Wireless Communications and Mobile Computing*, vol. 5, no. 2, pp. 123–137, Mar. 2005.
- [2] A. Scaglione, G. B. Giannakis, and S. Barbarossa, “Redundant filterbank precoders and equalizers. I. Unification and optimal designs,” *IEEE Trans. Signal Process.*, vol. 47, no. 7, pp. 1988–2006, July 1999.
- [3] G. Cherubini, E. Eleftheriou, and S. Olcer, “Filtered multitone modulation for very high-speed digital subscriber lines,” *IEEE Trans. Commun.*, vol. 20, no. 5, pp. 1016–1028, June 2002.
- [4] N. Benvenuto, S. Tomasin, and L. Tomba, “Equalization methods in OFDM and FMT systems for broadband wireless communications,” *IEEE Trans. Commun.*, vol. 50, no. 9, pp. 1413–1418, Sept. 2002.
- [5] B. Muquet, Z. Wang, G. B. Giannakis, M. de Courville, and P. Duhamel, “Cyclic prefixing or zero padding for wireless multicarrier transmissions?” *IEEE Trans. Commun.*, vol. 50, no. 12, pp. 2136–2148, Dec. 2002.
- [6] M. R. B. Shankar and K. V. S. Hari, “Reduced complexity equalization schemes for zero padded OFDM systems,” *IEEE Signal Process. Lett.*, vol. 11, no. 9, pp. 752–755, Sept. 2004.
- [7] F. D. Beaulieu and B. Champagne, “Multicarrier modulation using perfect reconstruction DFT filter bank transceivers,” in *Int. Conf. on Information, Comm. and Sig. Processing*, Bangkok, Thailand, Dec. 2005, pp. 111–115.
- [8] P. P. Vaidyanathan, *Multirate Systems and Filter Banks*. Prentice Hall, 1993.
- [9] S. Weiss and R. W. Stewart, “Fast implementation of oversampled modulated filter banks,” in *Electronics Letters*, vol. 36, no. 17, Aug. 2000, pp. 1502–1503.